

Low-energy e^- -CO scattering in the static-exchange approximation

Deborah A. Levin, Arne W. Fliflet, and Vincent McKoy

*A. A. Noyes Laboratory of Chemical Physics, * California Institute of Technology, Pasadena, California 91125*

(Received 21 February 1979)

This paper presents a theoretical study of e^- -CO scattering at collision energies from 1 to 7 eV in the static-exchange approximation. The T -matrix discrete-basis-set approach to electron-molecule scattering introduced by Rescigno, McCurdy, and McKoy is used together with the variational correction method of Fliflet and McKoy. The authors show the behavior of the $^2\Sigma$ and $^2\Pi$ channel eigenphases and extract the width and position of the $^2\Pi$ shape resonance. Comparison is made with other theoretical and semiempirical results and with the corresponding resonance parameters for e^- -N₂ scattering. The momentum-transfer cross section is calculated and compared with the experimental data of Land and with other theoretical results.

I. INTRODUCTION

Ab initio calculations are an important source of dynamical information for low-energy electron-molecule collision processes. The complexity of these calculations has limited applications for the most part to simple homonuclear diatomics such as H₂,^{1,2} N₂,^{3,4} and F₂.⁵ [cf. also Ref. (16)]. Elastic scattering by N₂ has received particular attention because the $^2\Pi_g$ shape resonance is characteristic of low-energy electron scattering by molecules.⁶ Several calculations have shown that the static-exchange approximation for the electron-molecule interaction potential accounts for most of the dynamical features of e^- -N₂ scattering even though polarization effects are not included.^{3,4,7} Advantages of the static-exchange approximation are that it involves no adjustable parameters, and it treats the exchange interaction correctly.

An important test of a theoretical model is the ability to reproduce correctly dynamical trends when applied to different systems. In this regard it is of interest to apply the static-exchange approximation to low-energy e^- -CO scattering, especially in light of the considerable theoretical attention given to the isoelectronic e^- -N₂ system. The absence of inversion symmetry in CO introduces important new dynamical features due to the strong coupling between odd and even partial waves and the presence of a permanent dipole moment. However, one expects a strong family resemblance between the cross sections and resonance parameters of these two isoelectronic systems. In the case of N₂ and CO, this has been verified experimentally, as discussed in a review by Schultz.⁶

More recently, experimental data for the momentum-transfer cross section of CO have been obtained by Land,⁸ and semiempirical results for the resonance parameters of the $^2\Pi$ resonance in CO have been obtained by Zubek and Szymkowski.⁹ Theoretical results for e^- -CO scattering have been

obtained by Chandra^{10,11} from a numerical close-coupling calculation which used a pseudopotential plus a semiempirical polarization potential.

This paper reports a theoretical study of low-energy e^- -CO scattering in the static-exchange approximation. The theoretical approach is the T -matrix discrete-basis-set method for electron-molecule scattering introduced by Rescigno, McCurdy, and McKoy,¹² and developed by McKoy and co-workers.^{4,13} This approach has been successfully applied to electron scattering by H₂ (Refs. 12–14) and N₂ (Refs. 4 and 7) in the static-exchange approximation. The method makes use of a separable form of the potential

$$V^t = \sum_{\alpha\beta} |\alpha\rangle\langle\alpha|V|\beta\rangle\langle\beta|, \quad (1)$$

where $\{|\alpha\rangle\}$ is a finite set of Gaussian functions. The scattering amplitude or the K matrix for the truncated potential V^t contains errors due to the difference $V - V^t$. These errors are corrected to first order by application of the variational formula for the partial-wave K matrix¹³

$$K_{l'l'm}^s = K_{l'l'm}^t + 2k\langle\psi_{kl'm}^t|(V - V^t)|\psi_{kl'm}^t\rangle, \quad (2)$$

where $\psi_{kl'm}^t$ is a scattering wave function for the potential V^t .

This study considers the energy region from 1 to 7 eV in which the scattering is dominated by short-range interactions. Thus, only low partial-wave elements of the K matrix are important, and the effect of the long-range dipole moment is small. Eigenphases and eigenphase sums are presented for the $^2\Sigma$ and $^2\Pi$ scattering symmetries. The width and position of the $^2\Pi$ shape resonance are obtained from the eigenphase sum. Comparison is made with the corresponding parameters for the $^2\Pi_g$ shape resonance in e^- -N₂ scattering. The momentum-transfer cross section is calculated in the fixed-nuclei approximation.

II. THEORY

In the fixed-nuclei approximation the Schrödinger equation for an elastically scattered electron is of the form

$$[-\nabla^2 + U(R, \vec{r}) - k^2] \psi_{\vec{r}}(R, \vec{r}) = 0, \quad (3)$$

where $U = 2V$ and R is the internuclear separation for a diatomic. Except as noted, atomic units are assumed throughout. The incident-direction dependence of the scattering wave function may be expanded in the partial-wave series

$$\psi_{\vec{r}}(\vec{r}) = \left(\frac{2}{\pi}\right)^{1/2} \sum_{l,m} i^l \psi_{klm}(\vec{r}) Y_{lm}^*(\vec{k}). \quad (4)$$

In the case of a linear target with internuclear axis along the z axis, ψ_{klm} may in turn be expanded in the partial-wave series

$$\psi_{klm}(\vec{r}) = \sum_{l'} g_{l'l'm}(k, r) Y_{l'm}(\hat{r}). \quad (5)$$

Equation (5) defines a set of radial continuum functions with the asymptotic form for standing-wave boundary conditions:

$$g_{l'l'm}(k, r) \rightarrow j_{l'}(kr) \delta_{l'l'} - K_{l'l'm} y_{l'}(kr) \quad (6)$$

as $r \rightarrow \infty$, where $j_{l'}(kr)$ and $y_{l'}(kr)$ are regular and irregular spherical Bessel functions.

The scaled K matrix

$$K' = -\frac{2K}{\pi} \quad (7)$$

satisfies the Lippmann-Schwinger equation

$$K' = U + U G_0^P K', \quad (8)$$

where G_0^P is the principal-value part of the free-particle Green's function. Inserting the separable potential $U^t = 2V^t$ into Eq. (8) leads to the finite matrix equation

$$\langle \alpha | K' | \beta \rangle = \langle \alpha | U | \beta \rangle + \sum_{\alpha\delta} \langle \alpha | U | \alpha \rangle \langle \alpha | G_0^P | \delta \rangle \times \langle \delta | K' | \beta \rangle \quad (9)$$

which has the solution

$$K'^t = (1 - U^t G_0^P)^{-1} U^t. \quad (10)$$

The on-shell partial-wave K matrix is obtained by the transformation

$$K_{l'l'm}^t = -k \sum_{\alpha\beta} \langle j_{l'} Y_{l'm} | \alpha \rangle \langle \alpha | K' | \beta \rangle \times \langle \beta | j_{l'} Y_{l'm} \rangle. \quad (11)$$

The solution K'^t corresponds to the wave function

$$\psi_{klm}^t = \phi_{klm} + G_0^P K'^t \phi_{klm}. \quad (12)$$

Introducing the single-center expansion

$$\psi_{klm}^t(\vec{r}) = \sum_{l'} g_{l'l'm}^t(k, r) Y_{l'm}(\hat{r}) \quad (13)$$

leads to the asymptotic form

$$\psi_{klm}^t \rightarrow \sum_{l'} (j_{l'} \delta_{l'l'} - y_{l'} K_{l'l'm}^t) Y_{l'm} \quad (14)$$

as $r \rightarrow \infty$. Thus ψ_{klm}^t satisfies the appropriate boundary conditions for use in the Kohn variational formula¹⁵ [Eq. (2)]. The distorted-wave-approximation form of Eq. (2) follows from the fact that the free-particle Green's function is not approximated in Eq. (12).¹³

The scattering amplitude in the laboratory frame (with the z' axis in the direction of the incident electron) has the single-center expansion (for a diatomic target)¹⁶

$$f_{\vec{k}}(\vec{R}', \hat{r}') = \sum_{l'l'mm'} a_{l'l'mm'}(k, R) D_{m'm}^{(l)}(\hat{R}') \times D_{0m}^{(l')}(\hat{R}') Y_{l'm}(\hat{r}'), \quad (15)$$

where \hat{R}' denotes the target orientation angles, and \hat{r}' denotes the scattering angles in the laboratory frame. The dynamical coefficients introduced by Temkin *et al.*¹⁶ are given by⁴

$$a_{l'l'm}(k, R) = i^{l'-l} [4\pi(2l'+1)]^{1/2} \sum_{l''} (1 - iK)_{l'l''m}^{-1} K_{l''l'm}. \quad (16)$$

The single-center expansions are defined with respect to the center of mass of the target.

In the fixed-nuclei approximation the total elastic cross section is given by¹⁶

$$\sigma_T = \sum_{l'l'm} \frac{|a_{l'l'm}|^2}{2l'+1}. \quad (17)$$

The momentum-transfer cross section is defined as

$$\sigma_m = \int d(\cos\theta) \frac{d\sigma}{d(\cos\theta)} (1 - \cos\theta),$$

where $d\sigma/d(\cos\theta)$ is the differential cross section per unit polar angle averaged with respect to target orientation. The momentum-transfer cross section may be expressed as^{4,10}

$$\sigma_m = 4\pi(A_0 - \frac{1}{3}A_1), \quad (18a)$$

where

$$A_L = \frac{1}{4\pi(2L+1)} \sum_{l'l'\lambda\lambda'} [(2l+1)(2\lambda+1)]^{1/2} (\lambda 0 0 | L 0) (l' \lambda' 0 0 | L 0) (\lambda m \mu | L m + \mu) (l' \lambda' m \mu | L m + \mu) a_{l'l'm} a_{\lambda\lambda'\mu}^*. \quad (18b)$$

Garrett¹⁷ and Takayanagi¹⁸ have shown that owing to the presence of a permanent dipole moment, which gives rise to a long-range r^{-2} potential, the total fixed-nuclei cross section diverges for heteronuclear molecules. The time-averaged field of a rotating dipole is zero; hence, one obtains finite total cross sections by taking account of the rotational motion of the target. As shown by Garrett,¹⁷ the divergence of Eq. (17) for polar molecules is due to the divergence of the forward-scattering cross section. The momentum-transfer cross section, however, has a weighting factor of $1 - \cos\theta$, which removes contributions from forward scattering. Chandra¹⁰ has proved that σ_m is finite for polar molecules in the fixed-nuclei approximation.

The width and position of a shape resonance in nonspherical potential scattering can be extracted from the eigenphase sum by applying the formula¹⁹

$$\Delta(k) = f(k) + \tan^{-1}[\frac{1}{2}\Gamma/(E_r - \frac{1}{2}k^2)], \quad (19a)$$

where Γ and E_r are the resonance width and position, and Δ is the eigenphase sum. The function $f(k)$ represents the nonresonant scattering and may be expanded in powers of k^2 :

$$f(k) = a_0 + \frac{1}{2}a_2k^2 + \frac{1}{4}a_4k^4 + \dots \quad (19b)$$

We use this functional form only in a narrow energy range about the resonance position. This expansion is not used in the sense of an effective-range expansion about zero energy. Such a form would not be a valid effective-range expansion, since the CO potential has long-range components.

The static-exchange potential for a closed-shell diatomic molecule is of the form

$$V = -\frac{Z_A}{|\mathbf{r} - \mathbf{A}|} - \frac{Z_B}{|\mathbf{r} - \mathbf{B}|} + \sum_{\sigma=1}^N (2J_{\sigma} - K_{\sigma}), \quad (20)$$

where the Coulomb operator

$$J_{\sigma}(\mathbf{r}) = \int d^3r' \frac{\phi_{\sigma}^*(\mathbf{r}')\phi_{\sigma}(\mathbf{r}')}{|\mathbf{r} - \mathbf{r}'|}, \quad (21)$$

and K_{σ} is the corresponding exchange operator. The nuclear charges are denoted by Z_A and Z_B , the nuclei are located at \mathbf{A} and \mathbf{B} , and N is the number of occupied orbitals ϕ_{σ} . The variational formula [Eq. (2)] involves the matrix elements

$$\langle \psi_{k'l'm}^t | U | \psi_{k'l'm}^t \rangle \text{ and } \langle \psi_{k'l'm}^t | U^t | \psi_{k'l'm}^t \rangle.$$

The latter is given by

$$\langle \psi_{k'l'm}^t | U^t | \psi_{k'l'm}^t \rangle = \langle j_l Y_{lm} | (K'^t G_0^P + 1) U^t (1 + G_0^P K'^t) | j_l Y_{l'm} \rangle \quad (22)$$

and involves only components of $K'G_0^P$ and U within the discrete-basis-set subspace. The matrix element

$$\langle \psi_{k'l'm}^t | U | \psi_{k'l'm}^t \rangle = \sum_{pq} \langle g_{l'm}^t Y_{pq} | (U^{(s)} - U^{(ex)}) | g_{l'm}^t Y_{pq} \rangle \quad (23)$$

is evaluated using single-center expansions of the Coulomb interaction and each occupied orbital:

$$\phi_{\sigma}(\mathbf{r}) = \sum_s \phi_{s\sigma}(r) Y_{s\sigma}(\hat{r}). \quad (24)$$

Expressions for $\langle g_{l'm}^t | U^{(t)} | g_{l'm}^t \rangle$, $U^{(t)} = U^{(s)}$, $U^{(ex)}$ are given in Ref. 20. The direct matrix element involves a multipole expansion of the static potential:

$$U^{(s)}(\mathbf{r}) = 2 \sum_{\lambda} V_{\lambda}(r) P_{\lambda}(\hat{r}), \quad (25)$$

where P_{λ} is a Legendre polynomial. A prescription for obtaining a numerical representation of the continuum orbital $g_{l'm}^t$ is given in Ref. 13.

III. CALCULATIONS AND RESULTS

The electronic configuration of the ground state of CO is

$$X^1\Sigma^+ 1\sigma^2 2\sigma^2 3\sigma^2 4\sigma^2 5\sigma^2 1\pi^4.$$

To construct the static-exchange potential we performed a self-consistent-field (SCF) calculation for the ground state at an internuclear separation of 2.132 a.u. The SCF basis set consisted of a (9s, 5p, d) set of primitive Gaussians on each nucleus contracted to (4s, 3p, d). The exponents and contraction coefficients of this basis, which are due to Dunning,²¹ are given in Table I. The dipole moment of the CO ground state in this basis is 0.196 a.u.

The truncated scattering potential U^t is constructed separately for the Σ and Π scattering symmetries.⁴ The scattering basis set includes the uncontracted Gaussians used to represent occupied orbitals of the same symmetry as well as more diffuse Gaussians. The scattering basis sets used in this calculation are listed in Table II.

Our prescription for the matrix element $\langle \psi_{k'l'm}^t | U | \psi_{k'l'm}^t \rangle$ involves single-center expansions of the occupied orbitals [Eq. (24)], the static potential [Eq. (25)], and the scattering functions [Eq. (13)]. To converge the static-potential matrix element, we included $s=0, \dots, 30$ in the expansion of each occupied orbital; $\lambda=0, \dots, 30$ in the expansion of the electronic part of the static potential; $\lambda=0, \dots, 60$ in the nuclear part; $l'=0, \dots, 30$ in the expansion of the scattering wave function. Evaluation of the exchange-potential matrix elements involves a fivefold sum over the expansion indices of the occupied orbitals, the Coulomb interaction, and the continuum functions. This summation over

TABLE I. Target basis set.^a

$\vec{A} = (0.0, 0.0, -1.218)$, C atomic center		
(ϕ, q, r)	α_i	C_i
(0, 0, 0)	4232.61	0.002 029
(0, 0, 0)	634.882	0.015 535
(0, 0, 0)	146.097	0.075 411 0
(0, 0, 0)	42.497 4	0.257 121
(0, 0, 0)	14.189 2	0.596 555
(0, 0, 0)	1.966 6	0.242 517
(0, 0, 0)	5.147 7	1.0
(0, 0, 0)	0.496 2	1.0
(0, 0, 0)	0.153 3	1.0
(1, 0, 0)	18.155 7	0.039 196
(1, 0, 0)	3.986 40	0.244 144
(1, 0, 0)	1.142 900	0.816 775 0
(1, 0, 0)	0.395 4	1.0
(1, 0, 0)	0.114 6	1.0
(0, 1, 0)	Same α_i 's and C_i 's as (1, 0, 0)	1.0
(0, 0, 1)	Same α_i 's and C_i 's as (1, 0, 0)	1.0
(0, 0, 2)	0.75	1.0
(1, 0, 1)	0.75	1.0
(0, 1, 1)	0.75	1.0
$\vec{A} = (0.0, 0.0, 0.9140)$, O atomic center		
(ϕ, q, r)	α_i	C_i
(0, 0, 0)	7816.54	0.002 031
(0, 0, 0)	1175.82	0.015 436
(0, 0, 0)	272.188	0.073 771 0
(0, 0, 0)	81.169 6	0.247 606
(0, 0, 0)	27.189 6	0.611 832
(0, 0, 0)	3.413 6	0.241 205 0
(0, 0, 0)	9.532 2	1.0
(0, 0, 0)	0.939 8	1.0
(0, 0, 0)	0.284 6	1.0
(1, 0, 0)	35.183 2	0.040 023
(1, 0, 0)	7.904	0.253 849
(1, 0, 0)	2.305 1	0.806 842
(1, 0, 0)	0.717 1	1.0
(1, 0, 0)	0.213 7	1.0
(0, 1, 0)	Same α_i 's and C_i 's as (1, 0, 0)	1.0
(0, 0, 1)	Same α_i 's and C_i 's as (1, 0, 0)	1.0
(0, 0, 2)	0.85	1.0
(1, 0, 1)	0.85	1.0
(0, 1, 1)	0.85	1.0

^aThe Cartesian Gaussian function is of the form

$$\mu_{pqr}^{\alpha_i \vec{A}} \equiv N_{pqr} (x - A_x)^p (y - A_y)^q \times (z - A_z)^r \exp(-\alpha_i |\vec{r} - \vec{A}|^2),$$

where N_{pqr} is a normalization factor. C_i denotes the contraction coefficient of the i th basis function.

partial-wave indices was truncated by means of a cutoff on the magnitude of individual terms in the expansion. This cutoff was typically of the order of 10^{-5} or 10^{-6} . The one- and two-electron radial integrals that occur in the expansions for $\langle \psi_{k_1 m}^t | U | \psi_{k_1' m} \rangle$ are evaluated by Simpson's rule quadrature. A variable mesh was used for these quadratures with the step size increased for lar-

TABLE II. Scattering-basis-set exponents.^{a,b}

$^2\Sigma$		
$\vec{A} = (0.0, 0.0, -1.218)$	$(\phi, q, r) = (0, 0, 0)$	$(0.0, 0.0, 0.9140)$
4232.610	7816.54	0.1
634.882	1175.82	0.05
146.097	273.188	0.025
42.497 4	81.169 6	0.012 5
14.189 2	27.189 6	0.005
1.966 6	3.413 6	
5.147 70	9.532 2	
0.496 20	0.939 80	
0.153 30	0.284 600	
$(\phi, q, r) = (0, 0, 1)$		
18.155 7	35.183 2	0.07
3.986 4	7.904	0.037 5
1.142 9	2.305 1	0.018 75
0.395 4	0.717 1	0.007 5
0.114 6	0.213 7	
$^2\Pi$		
$\vec{A} = (0.0, 0.0, -1.218)$	$(\phi, q, r) = (1, 0, 0)$	
18.155 7	35.183 2	0.08
3.986 4	7.904	0.048
1.142 9	2.305 1	0.029 0
0.650	0.717 1	0.017 3
0.359 4	0.4	0.01
0.20	0.213 7	0.006
0.114 6	0.1	0.002
$(\phi, q, r) = (1, 0, 1)$		
0.75	0.85	0.75
0.3	0.40	0.03
0.10	0.15	0.01

^aSee Table I for explanation of symbols.

^bThe contraction coefficients are unity for each basis function.

ger distances from the origin. The two sets of radial increments used in this calculation are presented in Table III. We used the finer mesh (grid B in Table III) to improve the numerical accuracy of the exchange radial integrals for Π -symmetry scattering in the energy region of the shape resonance. All other radial integrals were evaluated using grid A in Table III. The numerical accuracy of the variational correction matrix elements is most critical in the region of a resonance because the $\langle \psi^t | U | \psi^t \rangle$ and $\langle \psi^t | U^t | \psi^t \rangle$ tend to be large, and significant figures are lost in the difference. We estimate the uncertainty in the corrected K -matrix elements $K_{i' m}^t$ not associated with basis-set errors at about 15%. This uncertainty is due to truncation of partial-wave expansions and round-off error in the radial quadratures occurring in the evaluation of $\langle \psi_{k_1 m}^t | U | \psi_{k_1' m} \rangle$.

TABLE III. Step sizes for numerical integrations.

Grid A						
<i>i</i> th interval ^a	1	2	3	4	5	
<i>h_i</i> ^b	0.038 07	0.076 4	0.152 28	0.304 56	0.609 1	
<i>n_i</i> ^c	48	96	192	216	600	
Grid B						
<i>i</i> th interval	1	2	3	4	5	6
<i>h_i</i>	0.019 035	0.038 07	0.076 14	0.152 28	0.304 56	0.609 1
<i>n_i</i>	96	192	288	384	480	600

^aThe quadrature mesh is broken up into different step sizes.

^b*h_i* is the incremental step size for the *i*th interval and has units of a.u./point.

^c*n_i* is the number of points for the *i*th interval.

Figure 1 shows eigenphases and eigenphase sums for *s*-, *p*-, and *d*-wave scattering in the ${}^2\Sigma$ channel. Contributions from higher partial waves are small at the energies studied and have been neglected. Eigenphases obtained from matrix elements of the corrected *K* matrix, $K_{i'l'm}^s$, and from uncorrected *K*-matrix elements $K_{i'l'm}^t$ are shown. The eigenphases are labeled by the partial wave with largest mixing coefficient. Table IV gives the eigenphases and mixing coefficients obtained

from corrected ${}^2\Sigma$ symmetry *K*-matrix elements at several energies. In Fig. 1 the eigenphase sum and the "*sσ*" and "*pσ*" eigenphases extrapolate toward π radians at low energy, while the "*dσ*" eigenphase extrapolates toward zero. Comparison of corrected and uncorrected results shows that the variational correction tends to dampen oscillations in the uncorrected eigenphases due to basis-set truncation. It is interesting to note that the individual uncorrected eigenphases oscillate out of the phase with each other as a function of energy. The uncertainty in our results due to basis-set truncation is related to the difference between the corrected and uncorrected results. Rough estimates of this uncertainty are: 10% for the corrected *sσ* eigenphase, 20% for the *pσ* eigenphase, and a factor of 2 for the *dσ* eigenphase.

Results for ${}^2\Pi$ channel eigenphases obtained from *p*-, *d*-, and *f*-wave *K*-matrix elements are shown in Fig. 2. The difference between corrected and uncorrected results is smaller than in the ${}^2\Sigma$ channel. This is probably a consequence of the fact that discrete-basis-set methods are particularly appropriate for scattering via a resonance state. The assignment of eigenphases in the vicinity of a resonance is governed by the avoided-crossing rule for eigenphases.²² Table V lists the eigenphases shown in Fig. 2, together with their *p*- and *d*-wave mixing coefficients. The contribution from *f*-wave scattering is small and has been neglected. The mixing coefficients are defined by the relation

$$\psi_k(\eta_i^1) \cong |C_p^i| \psi_{kp1} \pm |C_d^i| \psi_{kd1}. \quad (26)$$

In the resonance region we assign the $|C_p| - |C_d|$ combination to the resonant eigenphase and the combination $|C_p| + |C_d|$ to the slowly varying eigenphase. Outside the resonance region the eigenphases are labeled by the partial wave with largest mixing coefficient. In analogy with N_2 we label the resonant eigenphase " $\eta_{d\pi}$ " and the nonresonant

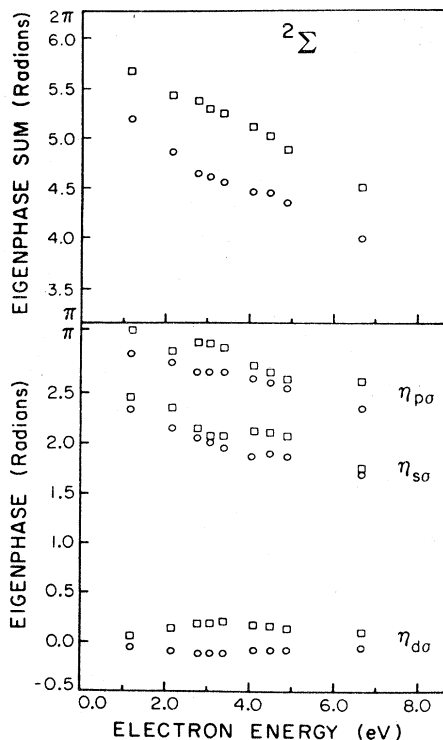


FIG. 1. Calculated eigenphases and the eigenphase sum for the ${}^2\Sigma$ channel. The circles represent the corrected and the squares represent the uncorrected results.

TABLE IV. Assignment of variationally corrected $^2\Sigma$ channel eigenphases (units of radians).

eV	$\eta_{s\sigma}$	C_s	C_p	C_d	$\eta_{p\sigma}$	C_s	C_p	C_d	$\eta_{d\sigma}$	C_s	C_p	C_d
1.2244	2.348	0.9939	-0.6013	0.0928	2.897	0.0517	0.9945	0.0905	-0.0559	-0.0976	-0.0852	0.9915
2.1768	2.158	0.9778	-0.1505	0.1453	2.801	0.1225	0.9751	0.1850	-0.1047	-0.169	-0.163	0.9719
3.40125	1.962	0.9576	-0.20199	0.2052	2.700	0.1925	0.9791	0.0656	-0.1057	-0.214	-0.0233	0.9765
4.8978	1.872	0.9117	-0.29007	0.2907	2.549	0.2706	0.9568	0.1061	-0.0662	-0.3089	-0.0180	0.9509
6.666	1.694	0.8797	-0.3393	0.333	2.349	0.3323	0.9397	0.07968	-0.0617	-0.340	-0.0406	0.9395

eigenphase " $\eta_{p\pi}$ ". Our results indicate that only one eigenphase shows resonance behavior even though p - d coupling is very strong in the resonance region.

Our results for the position and width of the Π shape resonance are given in Table VI. We give results extracted from the eigenphase sums of both uncorrected and corrected eigenphases through Eqs. (19a) and (19b). Our best result for the width of $\Gamma = 1.65 \pm 0.15$ eV is about twice the semiempirical result of Zubek and Symytkowski,⁹

which is also given in Table VI. Our best result for the position of 3.4 ± 0.1 eV is 1.5 eV higher than the semiempirical result.⁹ Results for the position and width of the $^2\Pi_g$ resonance of N_2 in static-exchange approximation⁷ are given in Table VI, together with the semiempirical results of Birtwistle and Herzenberg.²³ These results indicate that in N_2 the static-exchange approximation overestimates the width by a factor of ≈ 2 and puts the position about 1.5 eV above the best fit to experiment.²³ Thus the difference between static-exchange results and a semiempirical fit to experiment is about the same in CO and N_2 . We attribute this difference to the attractive polarization potential which generally lowers the position of a resonance and decreases its width.

Table VI includes theoretical results for the CO shape resonance obtained by Chandra¹¹ and for the N_2 shape resonance obtained by Chandra and Temkin.²⁴ The N_2 results of Ref. 24 are those of the fixed-nuclei calculations. Both these calculations use the numerical close-coupling approach and the pseudopotential method, in which exchange is approximately accounted for by imposing orthogonality conditions.²⁵ These calculations also include a semiempirical polarization potential which is "tuned" to give the resonance position correctly. The trend for the width shown by these results is in disagreement with those obtained from the static-exchange approximation and from semiempirical calculations: Chandra's width¹¹ for the CO resonance is smaller than Chandra and Temkin's²⁴ result for N_2 . In addition, Chandra's width for CO is a factor of 3 smaller than the semiempirical result of Zubek and Szmytkowski,⁹ even though polarization effects are included.

Figure 3 shows our static-exchange result for the total momentum-transfer cross section of CO. This cross section was obtained by including s -through f -wave scattering and is insensitive to contributions from higher partial waves. Figure 3 also shows the experimental results of Land⁸ and the pseudopotential plus semiempirical polarization results of Chandra.¹¹ In agreement with the resonance parameters given above, the resonance structure of σ_m in the static-exchange ap-

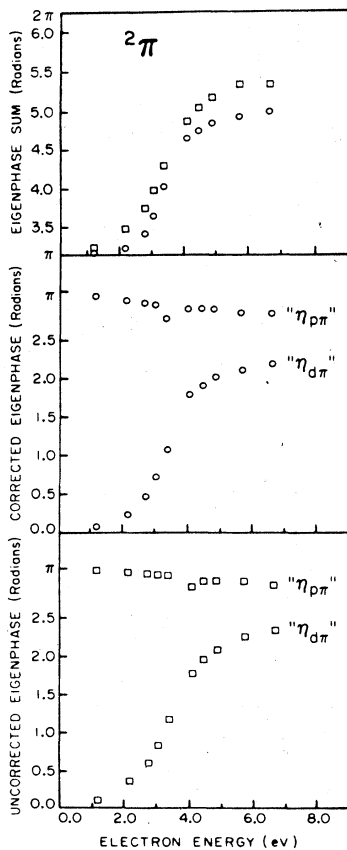


FIG. 2. Calculated eigenphases and the eigenphase sum for the $^2\Pi$ channel. The circles and squares follow the convention set in Fig. 1. See the text for the explanation of the assignment of individual eigenphases.

TABLE V. Assignment of variationally corrected Π -channel eigenphases.^a

eV	" η_{br} "	C_p	C_d	" η_{dr} "	C_p	C_d
1.2244	3.079	0.553	0.752	0.0696	0.789	-0.612
2.1768	3.0179	0.642	0.749	0.220	0.755	-0.655
2.755	2.991	0.723	0.681	0.462	0.683	-0.729
3.069	2.967	0.701	0.711	0.724	0.711	-0.703
3.4013	2.784	0.759	0.643	1.078	0.644	-0.764
4.1155	2.909	0.751	0.654	1.781	0.646	-0.756
4.4982	2.908	0.768	0.638	0.90	0.634	-0.769
4.8978	2.901	0.763	0.642	2.017	0.637	-0.767
5.748	2.870	0.783	0.555	2.108	0.592	-0.803
6.666	2.840	0.755	0.654	2.194	0.648	-0.755

^aGiven in units of radians.

proximation is broader than experimentally observed and is shifted to higher energy. The experimental resonance peak is about 50% higher than the static-exchange result. The static-exchange and experimental cross section are in good agreement above the resonance region. Our results for the momentum-transfer cross section are given in Table VII.

IV. DISCUSSION AND CONCLUSIONS

Our results show that the static-exchange approximation gives the correct trends in the resonance parameters of the isoelectronic systems N_2 and CO: The resonance in CO occurs at lower energy than in N_2 and has a larger width. Physically, these changes are expected because, unlike N_2 , the CO resonance contains p -wave as well as d -wave character. Thus the potential barrier, which is responsible for the shape resonance in both systems, is weaker in CO than in N_2 . We

TABLE VI. Comparison of CO and N_2 resonance parameters.

CO $^2\Pi$ resonance parameters in eV		
	E_r (eV)	Γ (eV)
Uncorrected T matrix	3.3 \pm 0.2	2.0 \pm 0.2
Corrected T matrix	3.4 \pm 0.1	1.65 \pm 0.15
Zubek <i>et al.</i> ^a	1.52 \pm 0.02	0.80 \pm 0.03
Chandra ^b	1.753	0.278
N_2 $^2\Pi_g$ resonance parameters in eV		
	E_r (eV)	Γ (eV) width
Corrected T matrix ^c	3.83 \pm 0.12	1.19 \pm 0.04
Birtwistle and Herzenberg ^d	1.925 \pm 0.015	0.57 \pm 0.02
Chandra and Temkin ^e	2.394	0.4

^aReference 9.^dReference 24.^bReference 11.^eReference 25.^cReference 7.

find that the effects of polarization are similar in CO and N_2 . The attractive polarization potential tends to lower the resonance energy and reduce the resonance width. We are studying a simple method of including polarization effects in our approach.²⁶

The behavior of the individual CO eigenphases is qualitatively similar to the behavior of the corresponding N_2 eigenphases, even though the coupling between partial waves is much stronger in CO. The $^2\Pi$ channel eigenphase sum clearly shows a resonance, but it passes through considerably less than π radians in the resonance region. This is due to significant contributions from nonresonant scattering. Chang²⁷ has shown that a model based on a single resonant eigenphase accounts for scattering via the $^2\Pi$ resonance in CO. Our results verify this model, at least for the static-exchange approximation. The

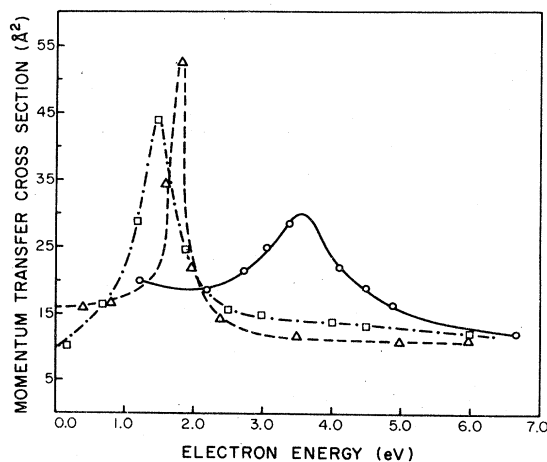


FIG. 3. Comparison of calculated momentum-transfer cross section (open circles) with the frame-transformation calculation of Chandra (Ref. 11) (open triangles) and the experimental results of Land (Ref. 8) (open squares).

TABLE VII. Momentum-transfer cross section (\AA^2).

Electron energy (eV)	σ_m
1.224	19.95
2.177	18.59
2.755	21.71
3.069	25.10
3.402	28.46
4.116	22.23
4.498	18.95
4.898	16.41
6.666	12.171

inclusion of polarization effects is unlikely to change this conclusion.

A discrete-basis-set expansion of the potential [Eq. (1)] is not expected to account accurately for the long-range component of the potential due a permanent dipole moment. In this calculation the effect of the CO dipole moment is included to first order by the variational correction [Eq. (22)]. This approach would not be appropriate at very low scattering energies ($\ll 1$ eV), but it should be adequate for the scattering processes considered

in this work. The scattering of low partial waves is dominated by short-range interactions, particularly when a resonance is involved. Moreover, the dipole moment of CO is relatively small.

Several discrete-basis-set methods for single-channel scattering from spherically symmetric potentials use the fact that basis set errors are minimized at eigenenergies of the basis-set representation of the Hamiltonian.²⁸ As discussed in previous work,⁴ improved uncorrected results can be obtained at eigenenergies for nonspherical potential scattering if the coupling is weak. Not surprisingly, this effect breaks down completely in CO due to the strong coupling: when the uncorrected "s" eigenphase is most accurate, the "p" eigenphase is least accurate, and conversely.

ACKNOWLEDGMENTS

This research was supported by Grant No. CHE76-05157 from the National Science Foundation and by an Institutional Grant from the U. S. Department of Energy, No. EY-76-G-03-1305. We would like to thank Dr. Land for the use of experimental results prior to publication.

*Contribution No. 5973

¹J. C. Tully and R. S. Berry, *J. Chem. Phys.* **51**, 2056 (1969).

²A. Klonover and U. Kaldor, *Phys. Rev. A* (to be published).

³M. A. Morrison and B. I. Schneider, *Phys. Rev. A* **16**, 1003 (1977).

⁴A. W. Fliflet, D. A. Levin, M. Ma, and V. McKoy, *Phys. Rev. A* **17**, 160 (1978).

⁵B. I. Schneider and P. J. Hay, *Phys. Rev. A* **13**, 2049 (1976).

⁶G. J. Schulz, *Rev. Mod. Phys.* **45**, 378 (1973).

⁷D. A. Levin and V. McKoy (unpublished).

⁸J. E. Land, *J. Appl. Phys.* **49**, 5716 (1978).

⁹M. Zubek and C. Szmytkowski, *J. Phys. B* **10**, L27 (1977).

¹⁰N. Chandra, *Phys. Rev. A* **12**, 2342 (1975).

¹¹N. Chandra, *Phys. Rev. A* **16**, 80 (1977).

¹²T. N. Rescigno, C. W. McCurdy, Jr., and V. McKoy, *Phys. Rev. A* **11**, 825 (1975).

¹³A. W. Fliflet and V. McKoy, *Phys. Rev. A* **18**, 2107 (1978).

¹⁴D. A. Levin, A. W. Fliflet, and V. McKoy, *Phys. Rev.*

A (to be published).

¹⁵W. Kohn, *Phys. Rev.* **74**, 1763 (1948).

¹⁶A. Temkin, K. V. Vasavada, E. S. Chang, and A. Silver, *Phys. Rev.* **186**, 57 (1969).

¹⁷W. R. Garrett, *Mol. Phys.* **24**, 465 (1972).

¹⁸K. Takayanagi, *Comments At. Mol. Phys.* **3**, 95 (1972).

¹⁹P. G. Burke and A. L. Sinfailam, *J. Phys. B* **3**, 641 (1970).

²⁰A. W. Fliflet and V. McKoy, *Phys. Rev. A* **18**, 1048 (1978).

²¹T. H. Dunning, Jr., *J. Chem. Phys.* **53**, 2823 (1970).

²²J. Macek, *Phys. Rev. A* **2**, 1101 (1970).

²³D. T. Birtwistle and A. Herzenberg, *J. Phys. B* **4**, 53 (1971).

²⁴N. Chandra and A. Temkin, *Phys. Rev. A* **13**, 188 (1976).

²⁵P. G. Burke and N. Chandra, *J. Phys. B* **5**, 1696 (1972).

²⁶D. A. Levin and V. McKoy (unpublished).

²⁷E. S. Chang, *Phys. Rev. A* **16**, 1850 (1977).

²⁸P. G. Burke, *Potential Scattering in Atomic Physics* (Plenum, New York, 1971), p. 75.